Immunity, Vol. 10, 547–558, May, 1999, Copyright ©1999 by Cell Press

Deficient T Cell Fate Specification in Mice with an Induced Inactivation of *Notch1*

Freddy Radtke,* Anne Wilson,†
Gerlinde Stark,* Michelle Bauer,‡
Joost van Meerwijk,†‖ H. Robson MacDonald,†
and Michel Aguet*§
*Swiss Institute for Experimental Cancer Research
1066 Epalinges
Switzerland
†Ludwig Institute for Cancer Research
Lausanne Branch
University of Lausanne
1066 Epalinges
Switzerland
‡Genentech, Incorporated
1 DNA Way
South San Francisco, California 94080

Summary

Notch proteins are cell surface receptors that mediate developmental cell specification events. To explore the function of murine Notch1, an essential portion of the gene was flanked with loxP sites and inactivation induced via interferon-regulated *Cre* recombinase. Mice with a neonatally induced loss of Notch1 function were transiently growth retarded and had a severe deficiency in thymocyte development. Competitive repopulation of lethally irradiated wild-type hosts with wild-type- and Notch1-deficient bone marrow revealed a cell autonomous blockage in T cell development at an early stage, before expression of T cell lineage markers. Notch1-deficient bone marrow did, however, contribute normally to all other hematopoietic lineages. These findings suggest that Notch1 plays an obligatory and selective role in T cell lineage induction.

Introduction

Maintenance of pluripotency, cell fate specification, and differentiation are processes that govern both embryonic development and homeostasis of self-renewing tissues throughout adulthood. Among the pathways that mediate such events, the Notch pathway has been extensively characterized in a number of developmental systems and shown to regulate cell fate specification (Artavanis-Tsakonas et al., 1995). This paradigm emerged notably from studies on embryonic neurogenesis in *Drosophila melanogaster*. The *Drosophila* nervous system is derived from equipotent precursor cells that can adopt two distinct cell fates to become either neuroblasts or neuroepidermal cells. Precursor cells express a set of basic helix-loop-helix transcription factors of the achaete-scute family. Notch activation results in repression of *achaete-scute* genes in a subset of precursor cells that consequently give rise to neuroepidermal cells. Accordingly, overexpression of Notch leads to an increase of neuroepidermal cells at the expense of neuroblasts, whereas lack of functional Notch protein leads to continued expression of the *achaete-scute* genes and thereby to an excess of neuroblasts (reviewed in Greenwald and Rubin, 1992; Ghysen and Dambly-Chaudiere, 1993; Artavanis-Tsakonas et al., 1995; Simpson, 1995).

Notch receptors are large conserved transmembrane proteins with ectodomains that contain up to 36 EGF-like repeats involved in ligand interaction (Rebay et al., 1991) and three copies of a cysteine-rich Lin-12/Notch (LN) motif of unknown function. Their cytoplasmic domains contain six ankyrin repeats that constitute a putative protein–protein interaction site and a C-terminal PEST sequence. Notch ligands are also membrane anchored and belong to the *Serrate*- or *Delta*-like gene family (Fehon et al., 1990; Fleming et al., 1990; Bettenhausen et al., 1995; Chitnis et al., 1995; Lindsell et al., 1995; Nye and Kopan, 1995; Shawber et al., 1996).

To date, four mammalian *Notch* homologs (*Notch1-4*) have been identified (Weinmaster et al., 1991, 1992; Reaume et al., 1992; del Amo et al., 1993; Lardelli and Lendahl, 1993; Lardelli et al., 1994; Uyttendaele et al., 1996). Vertebrate *Notch* genes are expressed in environments where cell fate changes take place. In addition to neuroepithelial tissue, *Notch* gene expression is found in the epidermis, in particular in hair follicles (Kopan and Weintraub, 1993), in dental epithelium (Mitsiadis et al., 1997), in the intestinal epithelium (Weinmaster et al., 1992), in hematopoietic precursors (Milner et al., 1994), and also in the thymus (Hasserjian et al., 1996).

The role of *Notch* family members in mammalian cell fate specification was explored both through gene overexpression and gene inactivation. The discovery of a chromosomal translocation in some human T lymphoblastic leukemias that resulted in a deletion of the ectodomain of the human *Notch1* gene, then designated *TAN-1* (Ellisen et al., 1991), suggested that Notch1 might thereby become constitutively activated. This observation stimulated a number of gain of function experiments in which a cytoplasmic domain of a Notch protein was expressed to activate the pathway. Thus, overexpression of the intracellular domain of mouse Notch1 resulted in repression of myogenesis in cultured cells (Kopan et al., 1994). Similarly, activated Notch1 prevented pluripotent embryonic carcinoma cells from differentiating into neurons but not into glia cells (Nye et al., 1994) and myeloid progenitor cells from differentiating into granulocytes (Milner et al., 1996). Cocultivation of fibroblastoid cells that expressed the Notch1 ligand Jagged with myoblasts that expressed Notch1 resulted in inhibition of myoblast differentiation (Lindsell et al., 1995). Altogether, these experiments did not allow it to distinguish between an instructive versus a permissive role of Notch signaling. That Notch1 is involved in mammalian cell fate determination was suggested by constitu-

§To whom correspondence should be addressed (e-mail: michel.aguet@isrec.unil.ch).
‖Present address: I. N. S. E. R. M., CHU-Papan, Toulouse CEDEX 31024, France.

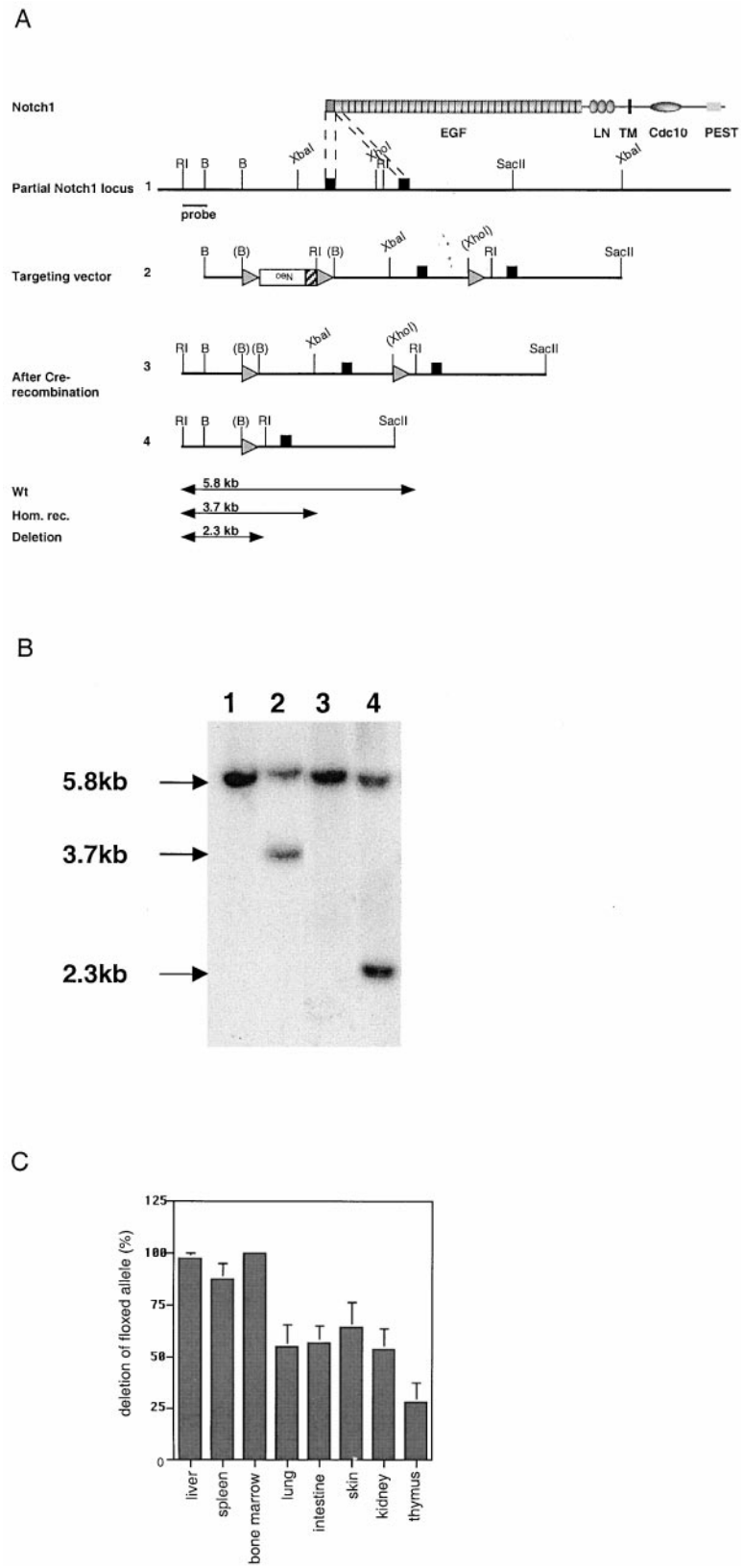

Figure 1. Inducible Targeting of the *Notch1* Gene

(A) Schematic representation of the murine Notch1 protein. The protein contains 2531 amino acid residues that encompass a signal peptide, 36 EGF repeats (EGF), a cystein-rich region (LN), a transmembrane domain (TM), cytoplasmic ankyrin repeats (Cdc10), and a PEST sequence. The genomic organization of the *Notch1* gene was determined only in part (1); black boxes, exons coding for the leader peptide and the first EGF repeat. Homologous recombination of the targeting vector introduced three loxP sites (filled triangles) plus a neomycin phosphotransferase gene (*PGK-neo*) into the *Notch1* locus (2), thereby flanking the exon coding for the leader peptide with two loxP sites. Transient transfection of *Cre*-recombinase into targeted ES cells resulted in three possible recombination events, two of which are illustrated: loss of the *PGK-neo* cassette only resulted in a *Notch1* locus in which a 3.7 kb gene segment harboring the exon coding for the signal peptide was flanked by two loxP sites (3); loss of the loxP-flanked segment containing the *PGK-neo* cassette plus the 3.5 kb *Notch1* gene portion resulted in the deletion of part of the putative *Notch1* promoter plus the exon encoding the signal peptide (4). Arrows indicate EcoRI fragments that differ in size between the wild-type locus (Wt) (1), the locus after homologous insertion of the targeting vector (2), and the locus after deleting the loxP-flanked 3.5 kb gene segment (4). RI, EcoRI; B, BamHI.

(B) Southern blot analysis of EcoRI-digested genomic ES-cell DNA. The probe indicated in (A) revealed a 5.8 kb fragment from the wild-type allele (lane 1). After homologous insertion of the replacement vector, the targeted allele gave rise to a 3.7 kb band (lane 2). Transient transfection of *Cre*-recombinase into the targeted ES cells resulting in the loss of the *PGK-neo* cassette only converted the 3.7 kb fragment into a 5.8 kb fragment (lane 3). The loss of the floxed 3.5 kb gene segment plus the *PGK-neo* cassette gave rise to a 2.3 kb band (lane 4). Lanes 1–4 correspond to the diagrams 1–4 in (A).

(C) Efficiency of Cre-recombinase-mediated *Notch1* deletion in various organs. Four 10-week-old *Notch1*$^{lox/lox}$*MxCre*$^{+/-}$ mice were injected four times i.p. at 2 day intervals with 300 μg of polyI-polyC. Genomic DNA from various tissues was prepared 2 days after the last injection and subjected to quantitative Southern blot hybridization (PhosphorImager). The deletion efficacy was calculated as the ratio of the signal from the inactivated allele to the total signal of the wild-type plus the inactivated allele and is expressed in percent.

tive activation of Notch1 in immature thymocytes that resulted in a biased CD4 versus CD8 lineage decision in favor of CD8 T cells as well as in a T cell receptor (TCR) expression that was skewed toward α/β TCRs (Robey et al., 1996; Washburn et al., 1997).

Inactivation of the mouse *Notch1* gene did not cause

gross developmental anomalies other than delayed and disorganized somitogenesis that resulted in embryonic lethality around day 10 of gestation (Swiatek et al., 1994; Conlon et al., 1995).

To explore the consequences of an inactivation of murine Notch1 beyond embryonic development, we made use of an interferon-inducible *Cre*-recombinase transgene (Kühn et al., 1995) to inactivate an essential loxP-flanked portion of the gene.

Results

Inducible Targeting of the *Notch1* Gene

To introduce loxP sites into the *Notch1* allele, ES cells (129Sv/Ev; Reis et al., 1994) were electroporated with a gene replacement vector containing a loxP-flanked neomycin phosphotransferase gene driven by the phosphoglycerate kinase promoter (*PGK-neo*) that was inserted 2.7 kb upstream of the initiation start site and a loxP site downstream of the exon encoding the signal peptide of Notch1 (Figure 1A). G-418-resistant colonies were screened by PCR and positive clones subjected to Southern blot analysis (Figure 1B, lanes 1 and 2). Targeted ES cell clones were transfected transiently with an expression vector encoding *Cre* recombinase under the control of the herpes simplex virus thymidine kinase promoter and individual clones assayed for the occurrence of two out of three possible recombination events (Figure 1A): (1) loss of the *PGK-neo* cassette alone, resulting in a *Notch1* allele in which the exon encoding the signal peptide was flanked by loxP sites; (2) loss of the *PGK-neo* cassette plus the 3.5 kb gene fragment, yielding a *Notch1* allele in which the exon encoding the signal peptide was deleted. Single colonies were screened by PCR and positives verified by Southern blot analysis. Loss of the *PGK-neo* cassette reverted the 3.7 kb EcoRI fragment, obtained through homologous recombination, to the wt 5.8 kb fragment (Figure 1B, lane 3), whereas loss of the *PGK-neo* cassette plus the 3.5 kb gene segment including the exon for the signal peptide resulted in a 2.3 kb fragment (Figure 1B, lane 4). Two independent ES-cell clones from each recombination event were used to generate chimeric founder males that were intercrossed with C57BL/6 females.

An alternative replacement vector was constructed in which the loxP-flanked *PGK-neo* cassette was placed immediately upstream of the translation initiation start within the 5′ UTR of the *Notch1* gene (data not shown). Mice derived from homologous insertion of this construct were also normal, indicating that the insertion of a loxP palindrome within the 5′ UTR of the *Notch1* gene had no significant effect on *Notch1* expression. The results presented herein were generated using the targeting strategy shown in Figure 1A. To ensure that the loss of the loxP-flanked exon would result in inactivation of the *Notch1* gene, mice heterozygous for the deletion of the exon encoding the signal peptide (*Notch1*$^{+/-}$) were intercrossed. From 101 offspring, no viable *Notch1*$^{-/-}$ mice were obtained. As reported (Swiatek et al., 1994; Conlon et al., 1995), all *Notch1*$^{-/-}$ mice died in utero around E9.5 of gestation (data not shown).

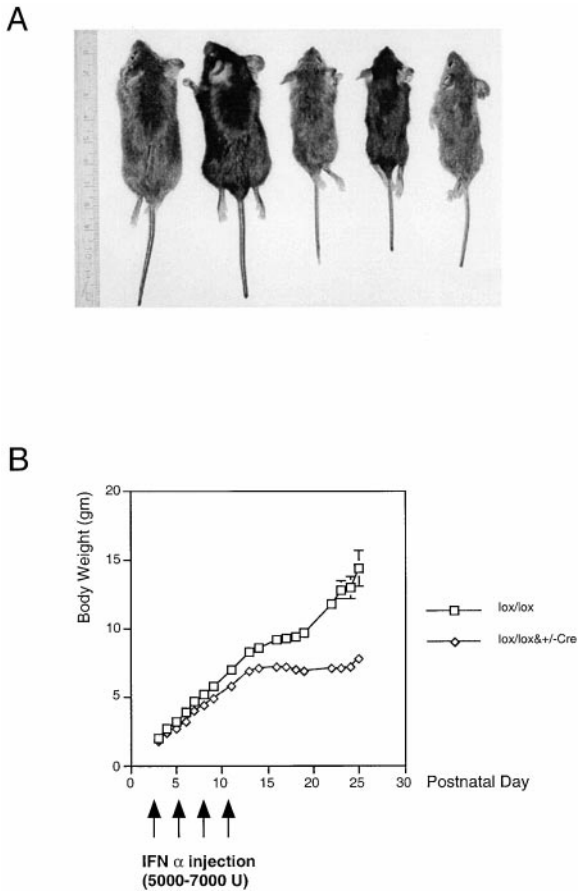

Figure 2. Inactivation of *Notch1* in Neonates Leads to Growth Retardation

(A) Comparison of the body size of five 4-week-old littermates treated with 5000–7000 U IFNα at days 3, 6, 9, and 11 after birth. Left: two control littermates (*Notch1*$^{lox/lox}$); right, three *iNotch1*$^{lox/lox}$ *MxCre*$^{+/-}$ littermates. Mice were genotyped at the age of 21 days. (B) Growth curve of one litter of six mice treated with IFNα as described in (A). n = 3 for controls (*Notch1*$^{lox/lox}$, open squares), and n = 3 for mutant mice (*Notch1*$^{lox/lox}$*MxCre*$^{+/-}$, open rectangles). Data shown are means ± SD.

Mice heterozygous for the loxP-flanked exon encoding the signal peptide (*Notch1*$^{+/lox}$) were bred to *Mx-Cre* transgenic mice harboring the *Cre-recombinase* transgene driven by the interferon-inducible *Mx* promoter (Kühn et al., 1995) and offspring intercrossed to generate *Notch1*$^{lox/lox}$*MxCre*$^{+/-}$ mice (heterozygous for the *Mx-Cre* transgene).

To assess the inducibility and efficacy of the *Notch1* inactivation, 3-month-old *Notch1*$^{lox/lox}$*MxCre*$^{+/-}$ mice received four intraperitoneal (i.p.) injections of the interferon inducer polyI-polyC at 2 day intervals. Two days after the last injection, genomic DNA from various tissues was prepared and the gene deletion efficiency quantified by Southern blot analysis (Figure 1C). The deletion efficiency was highest in the liver, spleen, and bone marrow (85% to 100%), whereas in the lung, intestine, skin, kidney, or thymus the deletion efficiency varied from 35% to 65%.

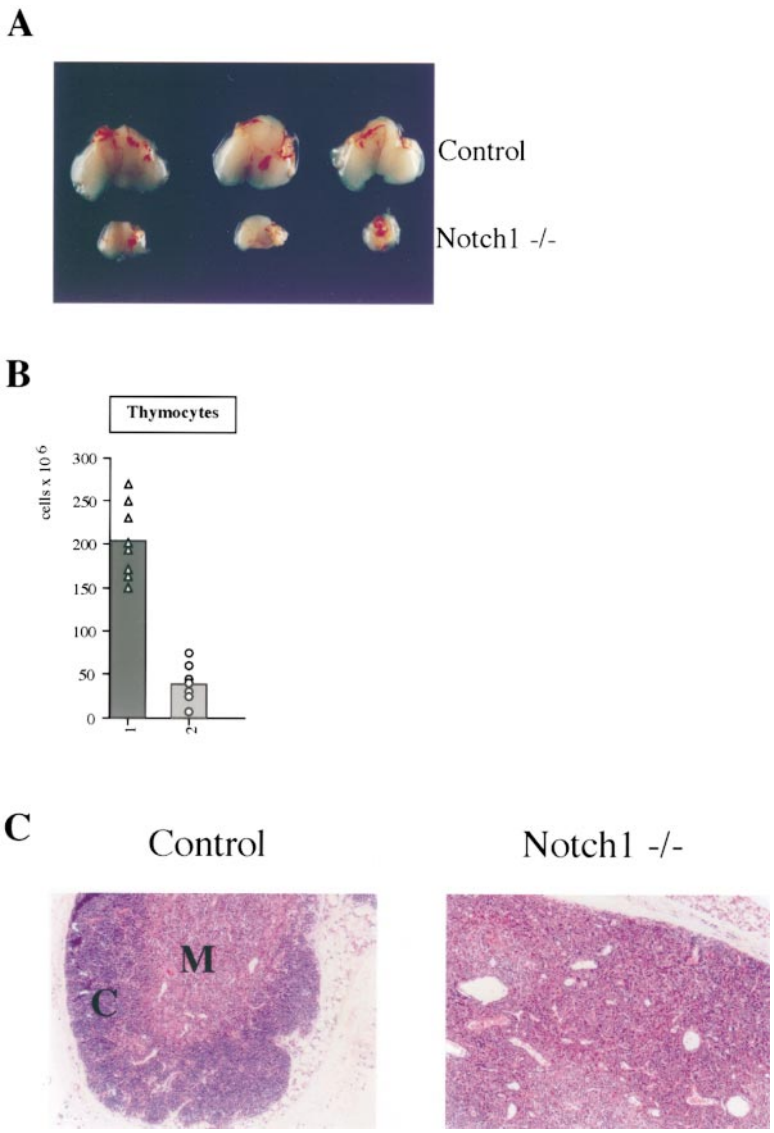

Figure 3. Abnormal Thymus Size and Morphology in *iNotch1*$^{-/-}$ Mice

(A) Freshly isolated thymus from 4-week-old *Notch1*$^{lox/lox}$ (control) versus *Notch1*$^{lox/lox}$ *MxCre*$^{+/-}$ mice. Littermates were injected neonatally with IFNα as described in Figure 2A. Seventeen days after the last IFNα injection, *iNotch1*$^{-/-}$ mice showed a marked reduction in thymus size.

(B) At the age of 4 weeks, *iNotch1*$^{-/-}$ mice showed a 5-fold reduction in thymocyte numbers. Numbers ($\times 10^6$) for control *Notch1*$^{lox/lox}$ (1) versus *Notch1*$^{lox/lox}$*MxCre*$^{+/-}$ mice (2) are shown as bar diagrams. Bars represent average values. Open triangles (control mice) and open circles (*iNotch1*$^{-/-}$ mice) represent values from individual mice. n = 8 for control; n = 11 for *iNotch1*$^{-/-}$ mice.

(C) Histological sections of the thymus of a 4-week-old *iNotch1*$^{-/-}$ and a control littermate stained with hematoxylin and eosin (magnification, ×100). M and C, medulla and cortex.

Induced Inactivation of *Notch1* in Newborn Mice Resulted in Growth Retardation and Abnormal Thymic Development

Notch1$^{lox/lox}$*MxCre*$^{+/-}$ mice were intercrossed and newborns injected i.p. with IFNα at days 3, 6, 9, and 11 after birth without knowledge of their genotype. Genotyping of *Notch1*$^{lox/lox}$ (control) versus *Notch1*$^{lox/lox}$*MxCre*$^{+/-}$ was performed 21 days after birth. IFNα-treated *Notch1*$^{lox/lox}$ *MxCre*$^{+/-}$ (hereafter *iNotch1*$^{-/-}$) mice showed reduced growth compared to IFNα-treated control *Notch1*$^{lox/lox}$ littermates (Figure 2A). During the first 2 weeks after birth, *iNotch1*$^{-/-}$ mice showed a weight gain similar to control littermates; however, they subsequently stabilized or decreased in weight, and some died for unknown reasons. Body weight was measured, and a representative growth curve from one litter consisting of three control and three *iNotch1*$^{-/-}$ mice is shown in Figure 2B. To rule out any contribution of the Cre recombinase to this phenotype, newborn wild-type or *Mx-Cre* transgenic mice were neonatally injected with IFNα. Growth curves were as for *Notch1*$^{lox/lox}$ controls (data not shown).

At 4 weeks of age, *iNotch1*$^{-/-}$ mice had a markedly smaller thymus (Figure 3A) with a 5-fold reduction in thymocyte numbers (Figure 3B) and an abnormal architecture where medullary and cortical regions could no longer be distinguished (Figure 3C).

Block in T Cell Development in *iNotch1*$^{-/-}$ Mice

To determine the stage at which the defect in thymic development occurred, cytofluorometric analysis of the CD4, CD8, and T cell receptor (TCR) phenotype was performed on thymocytes of *Notch1*$^{lox/lox}$ versus *iNotch1*$^{-/-}$ mice. Thymocytes from *iNotch1*$^{-/-}$ mice showed a moderate decrease in the percentages of mature single-positive CD4$^+$8$^-$ (CD4 SP) and CD4$^-$8$^+$ (CD8 SP) cells, a considerable decrease in CD4$^+$8$^+$ double-positive (DP) cells and a relative increase in CD4$^-$8$^-$ double-negative (DN) T cells (Figure 4A). In absolute terms, CD4 SP were reduced 5-fold, CD8 SP 4.4-fold, and DP thymocytes 9-fold, whereas the DN population remained largely unaffected. TCRγ/δ$^+$ DN thymocytes and immature single-positive thymocytes (ISP, defined by CD3^{low}CD4$^-$CD8$^+$)

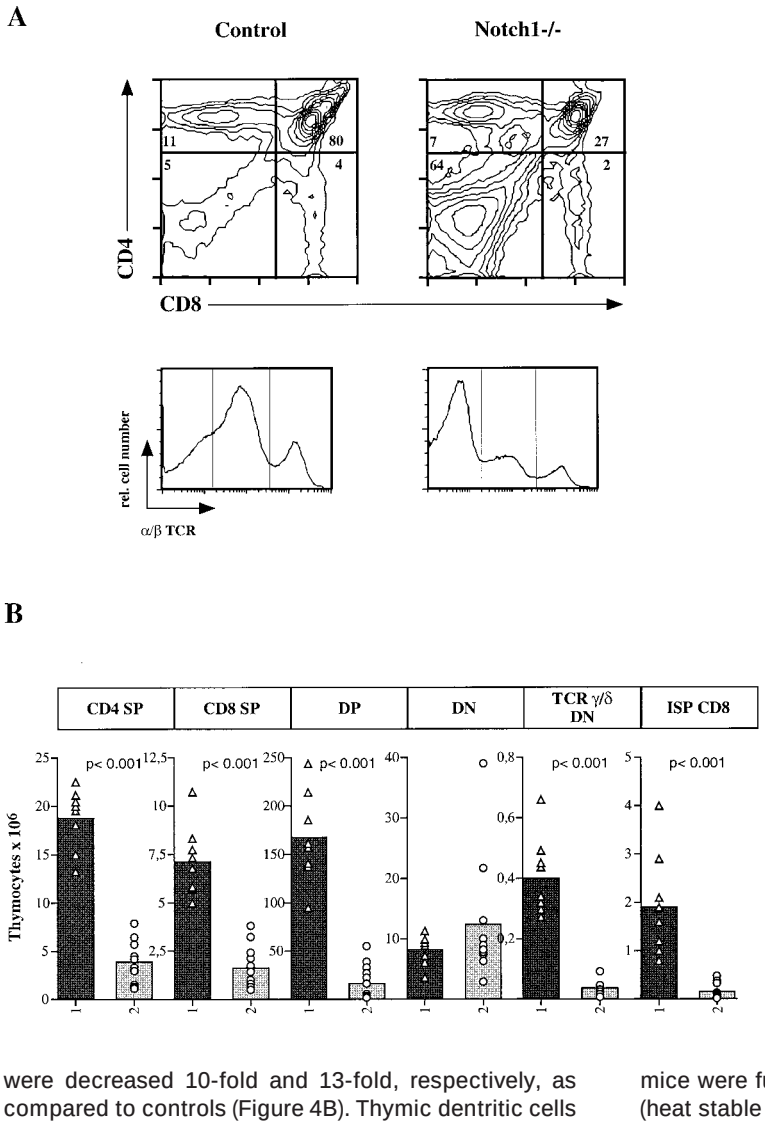

Figure 4. Reduction of T Cell Subsets in the Thymus of *iNotch1*$^{-/-}$ Mice

(A) The thymus was isolated from 4-week-old controls (*Notch1*$^{lox/lox}$) or *Notch1*$^{lox/lox}$*MxCre*$^{+/-}$ mice that were treated neonatally with IFNα as described in Figure 2A. The graph shows a FACS analysis of CD4 versus CD8 cells as well as histograms for TCR α/β expression for total thymocytes. Percentages of CD4 SP, CD4^{+}CD8^{+} (DP), CD8 SP, and CD4^{-}CD8^{-} (DN) cells are indicated in the quadrants.

(B) Absolute cell numbers (×10^{6}) for thymocyte subsets described in (A) were calculated and are shown as bar diagrams. The bars represent average values. Open triangles (control mice) and open circles (*iNotch1*$^{-/-}$ mice) represent values from individual mice. n = 8 for control; n = 11 for *iNotch1*$^{-/-}$ mice.

were decreased 10-fold and 13-fold, respectively, as compared to controls (Figure 4B). Thymic dentritic cells were reduced to a similar extent as DP thymocytes (data not shown).

To determine more precisely at what stage of thymocyte development the block occurred in *iNotch1*$^{-/-}$ mice, CD4^{-}8^{-} TCR^{-} (CD3^{-}) triple-negative (TN) thymocytes were analyzed for the expression of CD44 and CD25, which define distinct immature T cell populations (reviewed in Godfrey and Zlotnik, 1993). *iNotch1*$^{-/-}$ mice showed a block at or before the most immature T cell stage, as most TN thymocytes were CD44^{+}CD25^{-} (Figure 5A). While this population was increased 22-fold over the corresponding T cell population in control littermates, the more mature populations of CD44^{+}CD25^{+} and CD44^{-}CD25^{+} cells were reduced 11-fold and 26-fold, respectively (Figure 5B). CD44^{-}CD25^{-} cells were virtually undetectable in *iNotch1*$^{-/-}$ mice (data not shown).

Accumulation of B Cells in the Thymus of *iNotch1*$^{-/-}$ Mice

As expression of CD44 is not restricted to immature T cell progenitors but is also expressed on B cells and activated mature T cells, TN thymocytes from *iNotch1*$^{-/-}$ mice were further analyzed for the expression of CD24 (heat stable antigen, HSA), CD90 (Thy-1), CD117 (c-kit), and B220. CD24 is expressed on immature T cells and B cells, CD90 is found on all thymic T cells, CD117 on immature T cells, and B220 on B cells. Based on the expression of these markers, the most immature thymocytes in normal mice are defined as being CD44^{+} CD25^{-}CD24^{+}CD90$^{-/low}$CD117^{+}. Upon upregulation of CD25, these cells give rise to a CD44^{+}CD25^{+}CD24^{+} CD90^{low}CD117^{+} intermediate population that evolves to a CD44^{-}CD25^{+}CD24^{+}CD90^{+}CD117^{-} phenotype and eventually to the most mature TN population with downregulated CD25 (reviewed in Rodewald and Fehling, 1998). As shown in Figure 5C, over 90% of the CD44^{+} cells in *iNotch1*$^{-/-}$ mice coexpressed CD24 as compared to control littermates, where the majority of CD24^{+} cells were CD44^{-}. Only 2% of TN cells from *iNotch1*$^{-/-}$ mice expressed CD90 as compared to 75% in the controls. Within the CD44^{+} TN population, no CD117^{+} cells were detectable in *iNotch1*$^{-/-}$ mice, whereas controls had 50% CD117^{+} cells (data not shown).

Surprisingly, over 90% of this TN CD44^{+}CD25^{-}CD24^{+} CD90^{-}CD117^{-} cell population that was increased 22-fold in the thymus of *iNotch1*$^{-/-}$ mice (Figure 5B) were B220^{+}, compared to 10% in control mice (Figure 5C).

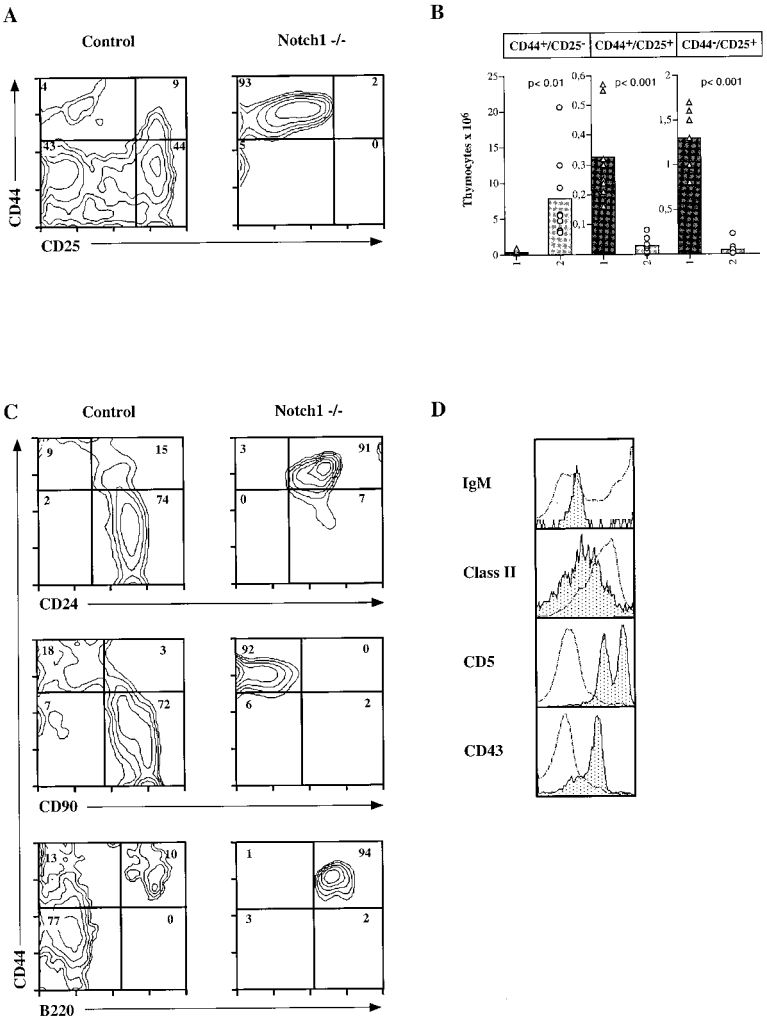

Figure 5. *iNotch1*$^{-/-}$ Mice Show a Developmental Arrest at the Stage of the Most Immature Thymocytes (CD44$^+$/CD25$^-$)

(A) Analysis of early thymocyte precursors in mutant and control mice. Thymocytes gated to eliminate cells expressing CD4, CD8, CD3ε, TCRα/β, and TCRγ/δ were stained for CD44 (Pgp-1) and CD25 (IL-2Rα). Percentages of the different subsets are indicated in the quadrants.

(B) Absolute cell numbers ($\times 10^6$) for the subsets described in (A) were calculated and are shown as bar diagrams. *iNotch1*$^{-/-}$ mice (2) show an accumulation in absolute cell numbers of the most immature thymocytes compared to control littermates (1). The bars represent average values. Open triangles (control mice) and open circles (*iNotch1*$^{-/-}$ mice) represent values from individual mice. The statistic significance was calculated using the Student's T-test; p-values are indicated above the bars. n = 8 for control; n = 8 for *iNotch1*$^{-/-}$ mice.

(C) Flow cytometric analysis of CD44, CD24, CD90, and B220 expression in 4-week-old *Notch1*$^{lox/lox}$ (controls) versus *Notch1*$^{lox/lox}$ *MxCre*$^{+/-}$ mice that were induced with IFNα as described in Figure 2A. Representative profiles of CD44 versus CD24, CD90, or B220 on thymocytes gated to eliminate cells expressing CD4, CD8, CD3ε, TCR α/β, and TCR γ/δ. Pecentages of the different T cell populations are indicated in the quadrants.

(D) Comparison of CD44$^+$/B220$^+$ gated thymocytes of control and *iNotch1*$^{-/-}$ mice stained with monoclonal antibodies specific for IgM, class II, CD5, and CD43. Controls, solid line, filled histogram; *iNotch1*$^{-/-}$ mice, dotted line.

Thus, altogether, B220$^+$ cells were approximately 200-fold increased in the thymus of *iNotch1*$^{-/-}$ mice as compared to controls. Thymic B220$^+$ cells from *iNotch1*$^{-/-}$ mice were further analyzed with regard to B cell–specific markers including IgM, major histocompatibility class II antigens (class II), CD5, and CD43, and compared to the small thymic B220$^+$ population found in littermate controls. In wild-type mice, thymic B cells represent around 0.2% of total thymic cells (Inaba et al., 1990). As shown in Figure 5D, IgM expression in thymic B220$^+$ cells of *iNotch1*$^{-/-}$ mice was biphasic as approximately half of the cells were IgM$^{-/low}$ and half IgM$^+$. Furthermore, B220$^+$ cells from *iNotch1*$^{-/-}$ mice were class II^{bright}, CD5^{low}, and CD43$^-$, as compared to the known class II intermediate, CD5$^+$, and CD43$^+$ phenotype in the controls (Miyama-Inaba et al., 1988). Thus, B cells found in thymus of *iNotch1*$^{-/-}$ mice differed in all four markers from normally occurring thymic B cells but resembled immature B cells normally found in the bone marrow (data not shown). Cytofluorometric staining patterns revealed no differences between bone marrow and peripheral lymph node B cells from *iNotch1*$^{-/-}$ versus control littermates (data not shown).

Evidence for a Cell Autonomous T Cell Differentiation Anomaly in *iNotch1*$^{-/-}$ Mice

To assess whether the abnormal thymic colonization observed in *iNotch1*$^{-/-}$ mice was due to the loss of Notch1 on thymocyte precursors or on thymic stromal cells, bone marrow from IFNα-treated control *Notch1*$^{lox/lox}$ or *iNotch1*$^{-/-}$ mice was transferred into lethally irradiated wild-type hosts. The *Notch1* gene was inactivated close to 100% in bone marrow cells from *iNotch1*$^{-/-}$ mice, as revealed by Southern blot analysis (Figure 6A, lanes 3 and 4 versus lanes 1 and 2). Chimeras were analyzed 6 months after transplantation. As shown in Figure 6B, thymic colonization was reminiscent of the thymic phenotype observed in newborn *iNotch1*$^{-/-}$ mice (Figure 4B).

While mature CD4 SP and CD8 SP were reduced 3-fold and DP thymocytes were reduced 4-fold, the DN thymocyte population was largely unaffected. TCRγ/δ$^+$ DN thymocytes as well as ISP cells were reduced 11-fold and 7-fold, respectively. The TN population revealed a developmental arrest at or before the stage of the earliest immature population (CD44$^+$CD25$^-$) (Figure 6C). Again, the majority of CD44-positive cells expressed

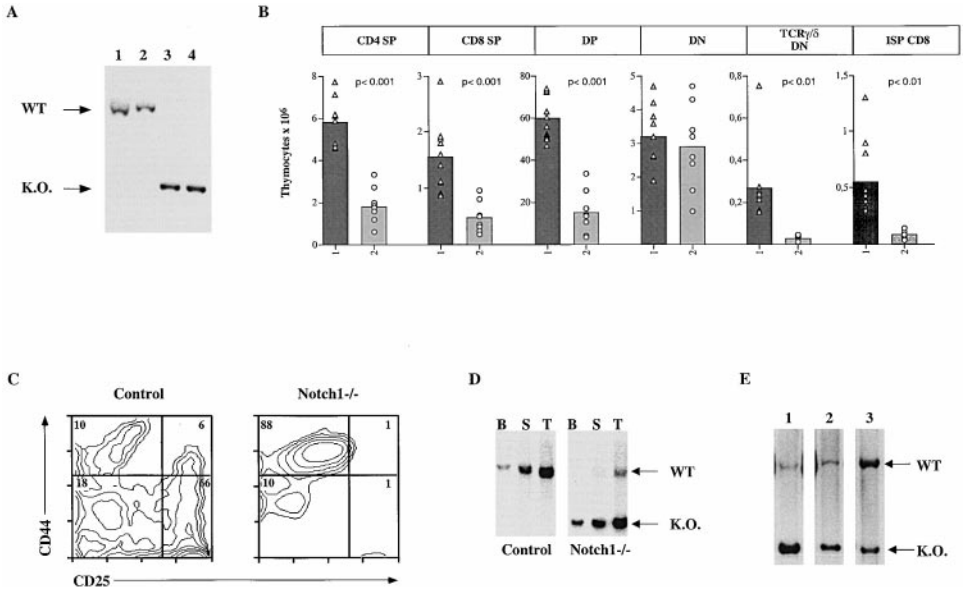

Figure 6. The Defect in T Cell Differentiation of *iNotch1*$^{-/-}$ Precursors Is Cell Autonomous

Two groups of six 12-week-old control mice (*Notch1*$^{lox/lox}$) and *Notch1*$^{lox/lox}$*MxCre*$^{+/-}$ received four i.p. injections of polyI-polyC (300 μg) at 2 day intervals. The bone marrow of these mice was used to reconstitute the immune system of lethally irradiated C57/Bl6 mice.

(A) Southern blot analysis of genomic DNA from pooled donor bone marrow from control (lanes 1 and 2, pool of three mice per lane) and *iNotch1*$^{-/-}$ mice (lanes 3 and 4, pool of three mice per lane). Genomic DNA was prepared 2 days after the last polyI-polyC injection. Notch1 mutant bone marrow showed close to a 100% recombination efficiency.

(B) The thymus of chimeric mice was analyzed 6 months after bone marrow transplantation. Cells were counted and stained with the indicated specific antibodies. Absolute cell numbers ($\times 10^6$) were calculated and are shown as bar diagrams. The bars represent average values. Open triangles (control donor bone marrow) and open circles (*iNotch1*$^{-/-}$ donor bone marrow) represent values from individual mice. The statistical significance was calculated using Student's T-test; p-values are indicated. n = 11 for chimeras transplanted with control bone marrow (1); n = 8 for chimeras transplanted with *iNotch1*$^{-/-}$ bone marrow (2).

(C) Phenotype of DN thymocytes in chimeric mice transplanted with control or *iNotch1*$^{-/-}$ bone marrow. Thymocytes were gated and stained as in Figure 5A.

(D) Southern blot analysis of genomic DNA from bone marrow (B), spleen (S), and thymus (T) of chimeras reconstituted with control or iNotch1$^{-/-}$ bone marrow. Conditions and probe see Figures 1A and 1B.

(E) Southern blot analysis of genomic DNA from the thymus of three individual chimeras reconstituted with *iNotch1*$^{-/-}$ bone marrow. Conditions and probe see Figures 1A and 1B.

B220, were biphasic for IgM expression, and were class II positive (data not shown), similar to the patterns observed in 4-week-old *iNotch1*$^{-/-}$ mice (Figures 5C and 5D). When bone marrow from control *Notch1*$^{lox/lox}$ mice was transplanted into lethally irradiated wild-type hosts, T cell development was unaffected (data not shown).

Even though thymic T cell development was affected similarly in neonatally induced *iNotch1*$^{-/-}$ mice and adult bone marrow chimeras grafted with *iNotch1*$^{-/-}$ bone marrow, the latter displayed only a moderate reduction in mature SP thymocytes. Southern blot analysis of the *Notch1* deletion in the bone marrow, spleen, and thymus of reconstituted chimeras indicated that the bone marrow was still entirely derived from *Notch1*-deleted cells (Figure 6D). Interestingly, however, the thymus seemed to have undergone a variable degree of repopulation from wild-type cells (10%-75%) during the 6 month recovery period, as evidenced by the detection of a *Notch1* wild-type restriction pattern (Figures 6D and 6E). To explore whether T cell maturation from residual wild-type precursors present in the *iNotch1*$^{-/-}$ donor cell population may have been favored, lethally irradiated hosts were reconstituted with bone marrow from *Notch1*$^{lox/lox}$ control or *iNotch1*$^{-/-}$ mice mixed in a 1:1 ratio with bone marrow from wild-type mice. The allelic markers CD45.2 and CD45.1, respectively, were used to distinguish the donor populations. Analysis of such mixed bone marrow chimeras 6 months after reconstitution revealed a complete absence in the thymus as well as in the periphery of any *iNotch1*$^{-/-}$ donor bone marrow–derived T cells (Figure 7). The distribution of the two allelic markers in lymph node cells pointed to an equivalent contribution of the different donor populations (Figure 7A, upper panel). While B220$^+$ cells were equally represented in wild-type and *iNotch1*$^{-/-}$ mice derived populations and while an expected proportion of CD3$^+$ cells was detected in the controls, CD3$^+$ cells derived from *iNotch1*$^{-/-}$ (CD45.2 tagged) precursors were undetectable (Figure 7A, lower panels). Similar results were obtained upon analysis of splenocytes and peripheral blood lymphocytes (data not shown). The thymus of mice repopulated with mixed wild-type (CD45.1 tagged) and *iNotch1*$^{-/-}$ (CD45.2 tagged) bone marrow was virtually devoid of CD45.2$^+$ cells (Figure 7B, upper panel) and the few residual cells proved to be B cells (Figure 7B, lower panels).

It is noteworthy that based on the staining of the

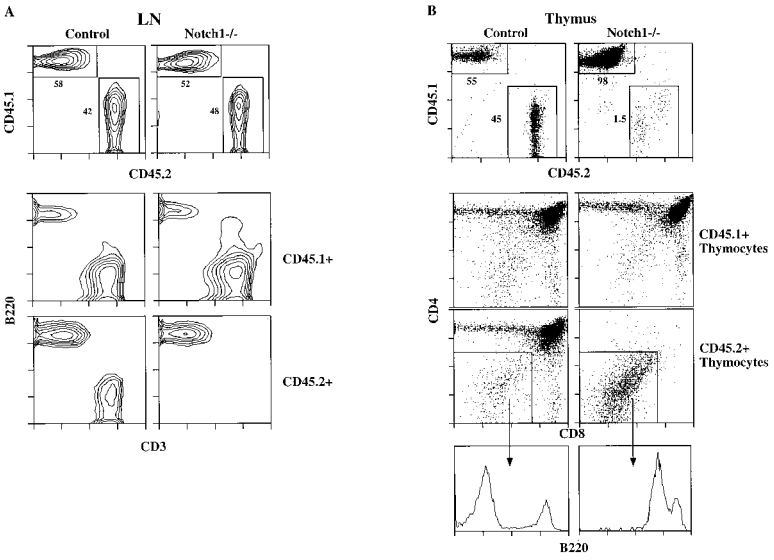

Figure 7. Competitive Repopulation of Lethally Irradiated C57/Bl6 Mice Reveals a Complete Inability of *iNotch1*$^{-/-}$ Bone Marrow to Generate T Cells

Two groups of five chimeric mice were analyzed 6 months after reconstitution with a 1:1 mixture of wild-type (CD45.1^{+}) and control (*Notch1*$^{lox/lox}$, *CD45.2*$^{+}$) or *iNotch1*$^{-/-}$ (*CD45.2*$^{+}$) bone marrow. Data are from representative chimeras in each group.

(A) FACS profile of lymph node cells stained with anti-CD45.1, anti-CD45.2, anti-B220, and anti-CD3 antibodies. The upper panel shows the relative contribution of the competing CD45.1 versus CD45.2 donor bone marrow–derived populations. The lower panel shows the distribution of CD3^{+} versus B220^{+} cells within the CD45.1^{+} or the CD45.2^{+} populations.

(B) FACS profile of thymocytes stained with anti-CD45.1, anti-CD45.2, anti-CD4, anti-CD8, and anti-B220 antibodies. The upper panel shows the relative contribution of the competing CD45.1 versus CD45.2 donor bone marrow–derived populations. The middle panel shows the distribution of CD4^{+} versus CD8^{+} cells within the CD45.1^{+} or the CD45.2^{+} populations, and the lower panel shows distribution of B220^{+} cells within the CD4^{-}CD8^{-} (DN) CD45.2^{+} population.

surface antigens Mac-1, GR1, Ter119, and NK1.1, both myeloid and erythroid lineages as well as NK cells derived from *iNotch1*$^{-/-}$ (CD45.2 tagged) bone marrow were normally represented (unpublished data).

Discussion

We report the initial phenotypic analysis of mice in which an essential portion of the *Notch1* gene was flanked by loxP sites (Figure 1A) and deleted inducibly through the activation of an interferon-responsive *Cre* recombinase transgene. To verify that the loxP-flanked portion of the *Notch1* gene was essential for its function, mice were generated from ES cell clones in which this portion was deleted upon transient expression of Cre recombinase. These *Notch1*$^{-/-}$ mice died around E9.5 with a phenotype described in earlier reports on constitutively inactivated mouse *Notch1* (Swiatek et al., 1994; Conlon et al., 1995). I.p. administration of either IFNα or polyI-polyC to *Notch1*$^{lox/lox}$*MxCre*$^{+/-}$ mice resulted in variable deletion of *Notch1* in different organs (Figure 1C). Consistent with previous observations (Kühn et al., 1995), the deletion was most efficient in the liver, spleen, and bone marrow.

To investigate the putative role of Notch1 in postnatal development, *Notch1*$^{lox/lox}$*MxCre*$^{+/-}$ mice were crossed with *Notch1*$^{lox/lox}$ mice and litters treated with IFNα. *Notch1*$^{lox/lox}$*MxCre*$^{+/-}$ offspring (*iNotch1*$^{-/-}$) but not IFNα-treated controls (*Notch1*$^{lox/lox}$) displayed a severe growth retardation (Figure 2). Although administration of high doses of IFNα to suckling mice was reported to be growth inhibitory and toxic (Gresser et al., 1975, 1981), the IFNα doses used to induce the gene deletion clearly had no detectable effect on controls. The observed growth retardation in *iNotch1*$^{-/-}$ mice was transient as these mice started to regain weight after an approximately 2 week stagnation period. However, even after 6 months, *iNotch1*$^{-/-}$ mice failed to reach the weight of their littermate controls. A similar phenotype was reported recently for mice that lack gelatinase B and showed a transient growth retardation due to abnormal skeletal growth plate vascularization and ossification (Vu et al., 1998). Interestingly, the *gelatinase B* promoter contains multiple putative binding sites for RBP-Jk that can associate with activated Notch1 to form a transcriptional activator of Notch target genes (Jarriault et al., 1995). The possibility that gelatinase B is under the control of Notch1 and might be functionally affected in *iNotch1*$^{-/-}$ mice is currently being explored.

Young *iNotch1*$^{-/-}$ mice showed a severe anomaly in thymocyte development. Loss of Notch1 during postnatal development led to a decrease of mature thymocytes of both α/β and γ/δ lineages, as well as developmentally intermediate (DP, ISP) and immature TN (CD4^{-}CD8^{-}CD3^{-}) thymocyte subsets (Figure 4), suggesting a developmental arrest at or before the most immature thymocyte precursor stage (CD44^{+}/CD25^{-}) (Figure 5).

A recently described lymphoid precursor population lacking myeloid differentiation potential has been defined as Lin^{-}IL-7R^{+}Thy1^{-}Sca1^{lo}CD117^{lo} (Kondo et al., 1997) and might be responsible for thymic colonization from the bone marrow. During thymus development, T lineage precursors differentiate along a complex developmental pathway and undergo a series of phenotypic changes that can be monitored by the differential expression of CD44 and CD25 (Godfrey and Zlotnik, 1993). The earliest precursor subset, expressing CD44 and CD117 but not CD25, has been shown to still have multipotential activity as it can give rise to T, B, NK, and dendritic cells (reviewed in Shortman and Wu, 1996). Subsequent subsets are defined as CD44^{+}CD25^{+}

$CD117^+$, $CD44^-CD25^+CD117^-$, and $CD44^-CD25^-CD117^-$ (reviewed in Godfrey and Zlotnik, 1993). Concurrent to these phenotypic changes, somatic recombination and transcriptional regulation of TCR genes, as well as proliferation of selected subsets, occurs (reviewed in Fehling and von Boehmer, 1997; Kang and Raulet, 1997; Rodewald and Fehling, 1998).

The presumed precursor population that accumulated in the thymus of *iNotch1*$^{-/-}$ mice resembled the earliest thymocyte precursor population ($CD44^+CD25^-$TN). However, these cells did not express thymocyte precursor markers such as CD117 and CD90 but instead expressed typical B cell markers such as B220, CD19, IgM, and MHC class II. Normally, thymic B cells represent only a small subset (0.2%) of thymic cells (Inaba et al., 1990). These thymic B cells that are found in the thymic medulla and have a specific phenotype ($B220^+IgM^{lo}$ $classII^{int}CD5^+CD43^+$) (Miyama-Inaba et al., 1988) that distinguishes them from peripheral B cells may play a role in negative T cell selection (Ferrero et al., 1999). The B cell population found in the thymus of *iNotch1*$^{-/-}$ mice differed in four out of five of these phenotypic markers (Figure 5D) and resembled B cells normally found in the bone marrow.

Intercellular interactions between precursor cells and the thymic stroma are essential for normal thymocyte development and maturation to occur (reviewed in Anderson et al., 1996). To clarify whether the aborted T cell development and the appearance of atypical B cells observed in the thymus of *iNotch1*$^{-/-}$ mice was due to a dysfunctional thymic microenvironment or to a cell autonomous defect at the level of immature precursors, bone marrow chimeras were generated using *iNotch1*$^{-/-}$ donor cells. These experiments largely recapitulated the observations made in young *iNotch1*$^{-/-}$ mice (Figure 6), suggesting that the developmental T cell arrest was indeed cell autonomous. The arrest proved incomplete, however, and a significant degree of T cell maturation was observed. Even though the gene deletion in the bone marrow of *iNotch1*$^{-/-}$ mice seemed complete (Figure 6D), it could not be ruled out that some precursor cells had escaped. Interestingly, Southern blot analysis of genomic DNA derived from bone marrow, spleen, or thymocytes 6 months after bone marrow transplantation revealed that the reconstituted bone marrow was entirely derived from *iNotch1*$^{-/-}$ cells, whereas the chimeric thymus contained an individually variable and occasionally abundant wild-type population (Figures 6D and 6E). After this period, radio-resistant host thymocytes have largely disappeared and were therefore ruled out as a source for the wild-type signal (Kadish and Basch, 1975; Ceredig and MacDonald, 1982). To assess whether residual wild-type thymocytes had expanded and matured to partially compensate for the *iNotch1*$^{-/-}$-mediated developmental arrest, lethally irradiated hosts were repopulated with mixed wild-type and *iNotch1*$^{-/-}$ bone marrow that was tagged with allelic markers (Figure 7). The analysis of such mixed chimeras 6 months after their reconstitution unequivocally revealed a virtually complete absence of any *iNotch1*$^{-/-}$-derived T cell lineages, both in the thymus and in the periphery. Thus, thymic T cell lineages beyond the $CD44^+/CD25^-$ stage observed in young *iNotch1*$^{-/-}$ mice (Figure 4) presumably did not mature in a Notch1-independent manner or escape because of redundant Notch signaling but were likely derived from cells that had already reached more mature stages at the time when *Notch1* was inactivated. T cell lineages in chimeras reconstituted with marrow *iNotch1*$^{-/-}$ (Figure 6) were likely derived from rare precursors that escaped Notch1 inactivation.

Notch1 protein is expressed at high levels in immature outer cortical $CD4^-CD8^-CD24^+$ thymocytes (Hasserjian et al., 1996), and several observations point to the involvement of Notch1-mediated signaling at different stages of T cell maturation, such as those leading to CD8 versus CD4 (Robey et al., 1996) and TCR γ/δ versus TCR α/β lineage choices (Washburn et al., 1997). Recently, an activated form of Notch1 was found to exhibit antiapoptotic properties that may be relevant for $CD4^+CD8^+$ DP thymocyte maturation (Deftos et al., 1998). Interestingly, an activated form of Notch1 introduced through a retrovirus into a stem cell containing population that was used for bone marrow reconstitution gave rise to clonal leukemias of exclusively immature T cell phenotypes (Pear et al., 1996). The data presented here suggest that Notch1 plays an essential role at an early developmental branch point when the T cell lineage is induced. It remains unclear in which compartment the absence of Notch1 affects this cell fate decision. Notch1$^{-/-}$-deficient lymphoid precursors (Kondo et al., 1997) could fail to respond to instructive signals within the stromal microenvironment of the bone marrow and/or fail to home to the thymus. Alternatively, these precursors may reach the thymus but fail to activate the Notch1 pathway in response to the thymic microenvironment and remain (inefficiently) directed toward a B cell fate. With the exception of their abnormal presence in the thymus, B cells seemed to develop normally in the absence of Notch1 signaling, since normal mature B cell phenotypes were observed in competitively repopulated lymph nodes (Figure 7A) as well as in the spleen and within peripheral blood lymphocytes (data not shown). Likewise, myeloid and erythroid lineages were generated in similar proportions from both wild-type and *iNotch1*$^{-/-}$-deficient bone marrow, suggesting that Notch1 is dispensable for hematopoiesis.

The molecular consequences of Notch1 inactivation in lymphoid precursors remain elusive. Both an instructive role for Notch1 in T cell fate induction or a permissive role for the outgrowth of T cell precursors are compatible with the phenotype reported here. The inducible inactivation model presented here should provide a novel basis for exploring the essential functions and molecular events of Notch1 signaling.

Experimental Procedures

Generation of Mice with a loxP-Flanked *Notch1* Allele

A genomic λ GEM-11 library (Müller et al., 1994) was screened using two pairs of overlapping oligonucleotides, muNotch1pr1u GTGGTG TGCGTCAACGTCCGATCCCCGCCGGCCACCCC, muNotch1pr1l CGGCGGCCTCTTGGGGTGGCCGGCGGGGATCGGACGTT and muNotch1pr2u TGCTCCCAGCCAAGTGGGACCTGCCTGAATGGA GGTAGG, muNotch1pr2l GGCCACTTCGCACCTACCTCCATTCAGG CAGGTCCCACT. A 12 kb genomic *Notch1* clone encompassing the exons coding for the leader peptide and the first EGF repeat was used to generate a 1.3 kb BamHI fragment containing the putative *Notch1* promoter region, a 3.5 kb BamHI–XhoI fragment containing

the exon coding for the leader peptide, and a 4.5 kb XhoI–SacII fragment including the exon encoding the first EGF repeat (Figure 1A). These fragments were cloned into the NotI, ASCI, and PmeI sites, respectively, of the TNLOX1-3 targeting vector. All loxP sites of the targeting vector were sequenced and the orientation of the inserts verified by restriction mapping and sequencing. Twenty micrograms of the targeting vector were linearized by SalI digestion and electroporated into the GS-1 embryonic stem cell line (Reis et al., 1994). Cells were subjected to G-418 selection (400 μg/ml), and single colonies were analyzed for homologous recombination of the targeting vector by PCR using Notch135JTGAGGCCTTTTCTTTTT GGAG and Neo-35KCGCCTTCTTGACGAGTTCTTC as primers. PCR positive colonies were verified by Southern blot analysis using a 750 bp BamHI–EcoRI fragment as a probe, derived from the 5′ upstream region of the Notch1 locus (Figure 1A). The frequency of homologous recombination events was 1:120. The complete integration of the 3′ region including the downstream loxP3 site was verified by PCR using loxP3-62WGGGTAGATAGGAGTAAGGGA CCA and loxP3-62V GTGTAGGGCTGAGCTCGAAAACC.

Three independent ES cell clones were transiently transfected with an expression vector encoding Cre-recombinase (pMC-Cre) generously provided by Werner Müller and Klaus Rajewsky, Cologne. One hundred colonies per ES-cell clone were screened by PCR and Southern blot analysis either for the loss of the PGK-neo cassette alone or the loss of the PGK-neo cassette plus the 3.5 kb gene segment. Primers used: PCR2 Cre loxP1-59T GATCGGCCGCC TCGAGATAAC and PCR2 Cre loxP1-59S GCCTACCTGCCATCCCG TCTG. Genomic DNA isolated from PCR positive colonies was digested with EcoRI and analyzed by Southern blotting using the 750 bp BamHI–EcoRI fragment as a probe (Figure 1A). ES cell clones in which the exon encoding the leader peptide was flanked by loxP sites or in which this exon was deleted were used to generate chimeric founder mice by microinjection into C57BL/6J blastocysts.

Heterozygous *Notch1*$^{lox/lox}$ mice were bred to *Mx-1-Cre* mice (Kühn et al., 1995) to generate *Notch1*$^{+/lox}$*MxCre*$^{+/-}$ mice that were intercrossed to generate *Notch1*$^{lox/lox}$*MxCre*$^{+/-}$ mice. Mice were genotyped for homozygosity of the loxP sites and the presence of the *Mx-1-Cre* transgene by PCR. Primers used: 5′ of loxP1 tv2 CTGACTT AGTAGGGGGAAAAC, 3′ of loxP1 tv2 AGTGGTCCAGGGTGTGAG TGT; generating a 350 bp fragment in the presence of a loxP site and a 300 bp fragment for the wt allele; Cre1 GGCCCCATGGCATCC AATTTACTGACCGTACAC, Cre2 TCGCTCGAGGTGATCGCCATCTT CCAGCAG, generating a 1 kb fragment.

Production of Murine IFN-α11

The cDNA encoding murine IFN-α11 was obtained by PCR from the pKCR6 vector kindly provided by Jeannine Doly (Civas et al., 1991), using the following primers: 5′ muIFN-α11 CCAACTGCAGTGCGATC TGCCTCACACTTATAACC and 3′ muIFN-α11 ACCGGAATTCCAGG ACTCAAGCCTTCTCTTCACTC. The c-DNA was subcloned into the pCR-Blunt Vector (Invitrogen) and further subcloned via EcoRI–PstI into the eucaryotic expression vector PS 262, which contained an in-frame Flag-tag (Schneider et al., 1997). This PS 262muIFN-α11 vector was used to generate stable 293 cell transfectants. These were grown for 3 weeks in 2 liter roller bottles, the medium filtered, and murine IFN-α11 purified over a Flag-column (Kodak) and concentrated using centricon 10 (Amicon). IFNα activity was determined using an antiviral assay in which murine L929 cells were challenged with vesicular stomatitis virus. The amount of IFNα that results in 50% protection from the cytopathic effect is defined as 1 U/ml.

Activation of the *Cre* Recombinase

Adult mice received four i.p. injections of 300 μg polyI-polyC (Sigma) at 2 day intervals. Two days after the last injection, mice were sacrificed and genomic DNA was prepared from various tissues. The deletion efficiency was assessed by Southern blot analysis of EcoRI-digested genomic DNA, hybridized with a 750 bp EcoRI–BamHI probe (Figure 1A). The analysis was quantified using a PhosphorImager (FUJI FILM BAS-1000). 5000–7000 units of murine IFN-α11 were administrated i.p. to newborn mice at day 3, 6, 9, and 11. At the age of 4 weeks, mice were sacrificed, and single cell suspensions of lymphocytes from thymus, spleen, lymph node, or bone marrow were prepared for FACS analysis.

Histological Analysis

The thymus from IFNα-treated control (*Notch1*$^{lox/lox}$) or *Notch1*$^{lox/lox}$ *MxCre*$^{+/-}$ mice was fixed in 4% paraformaldehyde for 4 hr and embedded in paraffin. Sections (4 μm) were stained with hematoxylin-eosin.

Flow Cytometry

Single cell suspensions of lymphocytes from thymus, spleen, lymph node, or bone marrow were prepared and stained for three- or four-color FACS analysis by standard procedures. Results were analyzed using either LYSYS II or CellQuest software on FACScan or FACS Calibur flow cytometers (Becton Dickinson), respectively. Most of the fluorescein, Cy-5, and biotin conjugates were prepared in one of our laboratories. These included anti-CD4 (GK 1.5), anti-CD8 (53.6.7), anti-CD25 (PC61.5), anti-CD44 (I. M.781), and anti-IgM (MB 86; Nishikawa et al., 1986). Anti-CD24 (M1/69), anti-CD3ε-FITC, anti-TCRβ-FITC and -PE, anti-TCRγ/δ-FITC, anti-B220-APC or -CyChrome, anti-CD44-CyChrome, anti-CD4-CyChrome, anti-CD8-APC, anti-CD43-FITC, anti-CD19-biotin, anti-class II-PE, anti-CD24-PE, and anti-CD5-PE conjugates were from PharMingen. PE-Streptavidin, CD25-PE, CD44-PE, B220-PE, and CD90-PE were from Caltag Laboratories. To analyze DN CD3$^-$ thymocytes, staining was performed using a pool of FITC direct conjugates (CD4, CD8, CD3, TCRα/β, and TCRγ/δ). Dead cells and debris were removed by appropriate gating of FSC and SSC.

Bone Marrow Chimeras

Bone marrow chimeras were generated using T cell–depleted bone marrow cells from IFNα-treated control (*Notch1*$^{lox/lox}$) or *Notch1*$^{lox/lox}$*MxCre*$^{+/-}$ mice. Ten-week-old hosts (C57BL/6L) were given 1000 rads of γ-irradiation 24 hr prior to receiving 5–10 × 10^6 donor bone marrow cells intravenously. Mixed chimeras were generated using a 1:1 mixture of T cell–depleted bone marrow cells from CD45.1$^+$ wild-type and CD45.2$^+$ *Notch1*$^{lox/lox}$ or *iNotch1*$^{-/-}$ mice. Radiation chimeras were maintained on antibiotic water and analyzed after 6 months.

Acknowledgments

We thank Rose Lees for help with generating bone marrow chimeras, Isabel Ferrero for dendritic cell analysis, Jeannine Bamat for histological work, and Werner Held for stimulating discussions. This work was supported in part by the Swiss National Science Foundation, the Veillon Foundation, and the Leenaards Foundation (G. S.).

Received April 8, 1999.

References

Anderson, G., Moore, N.C., Owen, J.J., and Jenkinson, E.J. (1996). Cellular interactions in thymocyte development. Annu. Rev. Immunol. *14*, 73–99.

Artavanis-Tsakonas, S., Matsuno, K., and Fortini, M.E. (1995). Notch signaling. Science *268*, 225–232.

Bettenhausen, B., Hrabe de Angelis, M., Simon, D., Guenet, J.L., and Gossler, A. (1995). Transient and restricted expression during mouse embryogenesis of Dll1, a murine gene closely related to Drosophila Delta. Development *121*, 2407–2418.

Ceredig, R., and MacDonald, H.R. (1982). Phenotypic and functional properties of murine thymocytes. II. Quantitation of host- and donor-derived cytolytic T lymphocyte precursors in regenerating radiation bone marrow chimeras. J. Immunol. *128*, 614–620.

Chitnis, A., Henrique, D., Lewis, J., Ish-Horowicz, D., and Kintner, C. (1995). Primary neurogenesis in Xenopus embryos regulated by a homologue of the Drosophila neurogenic gene Delta. Nature *375*, 761–766.

Civas, A., Dion, M., Vodjdani, G., and Doly, J. (1991). Repression of the murine interferon alpha 11 gene: identification of negatively acting sequences. Nucleic Acids Res. *19*, 4497–4502.

Conlon, R.A., Reaume, A.G., and Rossant, J. (1995). Notch1 is required for the coordinate segmentation of somites. Development *121*, 1533–1545.

Deftos, M.L., He, Y.W., Ojala, E.W., and Bevan, M.J. (1998). Correlating Notch signaling with thymocyte maturation. Immunity *9*, 777–786.

del Amo, F.F., Gendron-Maguire, M., Swiatek, P.J., Jenkins, N.A., Copeland, N.G., and Gridley, T. (1993). Cloning, analysis, and chromosomal localization of Notch-1, a mouse homolog of Drosophila Notch. Genomics *15*, 259–264.

Ellisen, L.W., Bird, J., West, D.C., Soreng, A.L., Reynolds, T.C., Smith, S.D., and Sklar, J. (1991). TAN-1, the human homolog of the Drosophila notch gene, is broken by chromosomal translocations in T lymphoblastic neoplasms. Cell *66*, 649–661.

Fehling, H.J., and von Boehmer, H. (1997). Early alpha beta T cell development in the thymus of normal and genetically altered mice. Curr. Opin. Immunol. *9*, 263–275.

Fehon, R.G., Kooh, P.J., Rebay, I., Regan, C.L., Xu, T., Muskavitch, M.A., and Artavanis-Tsakonas, S. (1990). Molecular interactions between the protein products of the neurogenic loci Notch and Delta, two EGF-homologous genes in Drosophila. Cell *61*, 523–534.

Ferrero, I., Anjuère, F., Martin, P., Martinez del Hoyo, G., Lopez Fraga, M., Wright, N., Varona, R., Marquez, G., and Ardavin, C. (1999). Functional and phenotypic analysis of thymic B cells: role in the induction of T cell negative selection. Eur. J. Immunol., *29*, 1598–1609.

Fleming, R.J., Scottgale, T.N., Diederich, R.J., and Artavanis-Tsakonas, S. (1990). The gene Serrate encodes a putative EGF-like transmembrane protein essential for proper ectodermal development in Drosophila melanogaster. Genes Dev. *4*, 2188–2201.

Ghysen, A., and Dambly-Chaudiere, C. (1993). The specification of sensory neuron identity in Drosophila. Bioessays *15*, 293–298.

Godfrey, D.I., and Zlotnik, A. (1993). Control points in early T-cell development. Immunol. Today *14*, 547–553.

Greenwald, I., and Rubin, G.M. (1992). Making a difference: the role of cell-cell interactions in establishing separate identities for equivalent cells. Cell *68*, 271–281.

Gresser, I., Tovey, M.G., Maury, C., and Chouroulinkov, I. (1975). Lethality of interferon preparations for newborn mice. Nature *258*, 76–78.

Gresser, I., Aguet, M., Morel-Maroger, L., Woodrow, D., Puvion-Dutilleul, F., Guillon, J.C., and Maury, C. (1981). Electrophoretically pure mouse interferon inhibits growth, induces liver and kidney lesions, and kills suckling mice. Am. J. Pathol. *102*, 396–402.

Hasserjian, R.P., Aster, J.C., Davi, F., Weinberg, D.S., and Sklar, J. (1996). Modulated expression of notch1 during thymocyte development. Blood *88*, 970–976.

Inaba, K., Hosono, M., and Inaba, M. (1990). Thymic dendritic cells and B cells: isolation and function. Int. Rev. Immunol. *6*, 117–126.

Jarriault, S., Brou, C., Logeat, F., Schroeter, E.H., Kopan, R., and Israel, A. (1995). Signalling downstream of activated mammalian Notch. Nature *377*, 355–358.

Kadish, J.L., and Basch, R.S. (1975). Thymic regeneration after lethal irradiation evidence for an intra-thymic radioresistant T cell precursor. J. Immunol. *114*, 452–458.

Kang, J., and Raulet, D.H. (1997). Events that regulate differentiation of alpha beta TCR+ and gamma delta TCR+ T cells from a common precursor. Semin. Immunol. *9*, 171–179.

Kondo, M., Weissman, I.L., and Akashi, K. (1997). Identification of clonogenic common lymphoid progenitors in mouse bone marrow. Cell *91*, 661–672.

Kopan, R., and Weintraub, H. (1993). Mouse notch: expression in hair follicles correlates with cell fate determination. J. Cell Biol. *121*, 631–641.

Kopan, R., Nye, J.S., and Weintraub, H. (1994). The intracellular domain of mouse Notch: a constitutively activated repressor of myogenesis directed at the basic helix-loop-helix region of MyoD. Development *120*, 2385–2396.

Kühn, R., Schwenk, F., Aguet, M., and Rajewsky, K. (1995). Inducible gene targeting in mice. Science *269*, 1427–1429.

Lardelli, M., and Lendahl, U. (1993). Motch A and motch B—two mouse Notch homologues coexpressed in a wide variety of tissues. Exp. Cell Res. *204*, 364–372.

Lardelli, M., Dahlstrand, J., and Lendahl, U. (1994). The novel Notch homologue mouse Notch 3 lacks specific epidermal growth factor-repeats and is expressed in proliferating neuroepithelium. Mech. Dev. *46*, 123–136.

Lindsell, C.E., Shawber, C.J., Boulter, J., and Weinmaster, G. (1995). Jagged: a mammalian ligand that activates Notch1. Cell *80*, 909–917.

Milner, L.A., Kopan, R., Martin, D.I., and Bernstein, I.D. (1994). A human homologue of the Drosophila developmental gene, Notch, is expressed in CD34+ hematopoietic precursors. Blood *83*, 2057–2062.

Milner, L.A., Bigas, A., Kopan, R., Brashem-Stein, C., Bernstein, I.D., and Martin, D.I. (1996). Inhibition of granulocytic differentiation by mNotch1. Proc. Natl. Acad. Sci. USA *93*, 13014–13019.

Mitsiadis, T.A., Henrique, D., Thesleff, I., and Lendahl, U. (1997). Mouse Serrate-1 (Jagged-1): expression in the developing tooth is regulated by epithelial-mesenchymal interactions and fibroblast growth factor-4. Development *124*, 1473–1483.

Miyama-Inaba, M., Kuma, S., Inaba, K., Ogata, H., Iwai, H., Yasumizu, R., Muramatsu, S., Steinman, R.M., and Ikehara, S. (1988). Unusual phenotype of B cells in the thymus of normal mice. J. Exp. Med. *168*, 811–816.

Müller, U., Steinhoff, U., Reis, L.F., Hemmi, S., Pavlovic, J., Zinkernagel, R.M., and Aguet, M. (1994). Functional role of type I and type II interferons in antiviral defense. Science *264*, 1918–1921.

Nishikawa, S., Sasaki, Y., Kina, T., Amagai, T., and Katsura, Y. (1986). A monoclonal antibody against Igh6-4 determinant. Immunogenetics *23*, 137–139.

Nye, J.S., and Kopan, R. (1995). Developmental signaling. Vertebrate ligands for Notch. Curr. Biol. *5*, 966–969.

Nye, J.S., Kopan, R., and Axel, R. (1994). An activated Notch suppresses neurogenesis and myogenesis but not gliogenesis in mammalian cells. Development *120*, 2421–2430.

Pear, W.S., Aster, J.C., Scott, M.L., Hasserjian, R.P., Soffer, B., Sklar, J., and Baltimore, D. (1996). Exclusive development of T cell neoplasms in mice transplanted with bone marrow expressing activated Notch alleles. J. Exp. Med. *183*, 2283–2291.

Reaume, A.G., Conlon, R.A., Zirngibl, R., Yamaguchi, T.P., and Rossant, J. (1992). Expression analysis of a Notch homologue in the mouse embryo. Dev. Biol. *154*, 377–387.

Rebay, I., Fleming, R.J., Fehon, R.G., Cherbas, L., Cherbas, P., and Artavanis-Tsakonas, S. (1991). Specific EGF repeats of Notch mediate interactions with Delta and Serrate: implications for Notch as a multifunctional receptor. Cell *67*, 687–699.

Reis, L.F.L., Ruffner, H., Stark, G., Aguet, M., and Weissmann, C. (1994). Mice devoid of interferon regulatory factor 1 (IRF-1) show normal expression of type I interferon genes. EMBO J. *13*, 4798–4806.

Robey, E., Chang, D., Itano, A., Cado, D., Alexander, H., Lans, D., Weinmaster, G., and Salmon, P. (1996). An activated form of Notch influences the choice between CD4 and CD8 T cell lineages. Cell *87*, 483–492.

Rodewald, H.R., and Fehling, H.J. (1998). Molecular and cellular events in early thymocyte development. Adv. Immunol. *69*, 1–112.

Schneider, P., Bodmer, J.L., Holler, N., Mattmann, C., Scuderi, P., Terskikh, A., Peitsch, M.C., and Tschopp, J. (1997). Characterization of Fas (Apo-1, CD95)-Fas ligand interaction. J. Biol. Chem. *272*, 18827–18833.

Shawber, C., Boulter, J., Lindsell, C.E., and Weinmaster, G. (1996). Jagged2: a serrate-like gene expressed during rat embryogenesis. Dev. Biol. *180*, 370–376.

Shortman, K., and Wu, L. (1996). Early T lymphocyte progenitors. Annu. Rev. Immunol. *14*, 29–47.

Simpson, P. (1995). Developmental genetics. The Notch connection. Nature *375*, 736–737.

Swiatek, P.J., Lindsell, C.E., del Amo, F.F., Weinmaster, G., and Gridley, T. (1994). Notch1 is essential for postimplantation development in mice. Genes Dev. *8*, 707–719.

Uyttendaele, H., Marazzi, G., Wu, G., Yan, Q., Sassoon, D., and Kitajewski, J. (1996). Notch4/int-3, a mammary proto-oncogene, is

an endothelial cell-specific mammalian Notch gene. Development *122*, 2251–2259.

Vu, T.H., Shipley, J.M., Bergers, G., Berger, J.E., Helms, J.A., Hanahan, D., Shapiro, S.D., Senior, R.M., and Werb, Z. (1998). MMP-9/gelatinase B is a key regulator of growth plate angiogenesis and apoptosis of hypertrophic chondrocytes. Cell *93*, 411–422.

Washburn, T., Schweighoffer, E., Gridley, T., Chang, D., Fowlkes, B.J., Cado, D., and Robey, E. (1997). Notch activity influences the $\alpha\beta$ versus $\gamma\delta$ T cell lineage decision. Cell *88*, 833–843.

Weinmaster, G., Roberts, V.J., and Lemke, G. (1991). A homolog of Drosophila Notch expressed during mammalian development. Development *113*, 199–205.

Weinmaster, G., Roberts, V.J., and Lemke, G. (1992). Notch2: a second mammalian Notch gene. Development *116*, 931–941.